

# Analysis of Temperature Dependence of GaAs DHBT Terminal Resistances Using the Observed Kink Effect

C. N. Dharmasiri, V. T. Vo, K. A. Koon, A. A. Rezazadeh

The Electromagnetic Centre, Dept of Electrical Engineering and Electronics, The University of Manchester, Manchester, PO BOX 88, M60 1QD, UK

**Abstract** — Large parasitic series resistances of heterojunction bipolar transistor (HBT) are shown to cause a sharp kink in the base current ( $I_B$ ) of the Gummel plot at elevated temperatures under high collector currents ( $I_C$ ) and low base-collector ( $b-c$ ) applied bias ( $V_{BC}$ ). This effect was analyzed and attributed to the temperature dependence of low-field and high field mobilities of undepleted and depleted areas at the  $b-c$  region. Using this observed kink a simple technique is presented to extract terminal resistances variation with temperature for an InGaP/GaAs DHBT. These extracted values are compared and verified with those extracted from  $s$ -parameter measurements. By incorporating these values into a temperature-dependent large signal DHBT model more accurate thermal behavior of  $I_B$  at high current is demonstrated.

## I. INTRODUCTION

Wireless communication systems require high-frequency power amplifiers, which perform efficiently in wide-ranging thermal environments. To accomplish this designers require more physically meaningful device models as well as greater understanding of their semiconductor material processes. When PA's are subjected to high power levels, the transistors typically operate under elevated junction temperatures that may thermally trigger undesirable effects such as increase in parasitic resistances.

Large series resistances in HBTs are shown to cause the  $b-c$  junction to become forward biased when operated under high  $I_C$ . This causes a sharp increase in  $I_B$ . Tiwari first reported this effect in the study of AlGaAs/GaAs DHBTs and demonstrated that by applying reverse bias to  $b-c$  junction the kink effect can be minimized [1]. In our earlier work [2] we also observed the same effect for an InGaP/GaAs SHBT and showed that by reverse biasing steps one can deduce the terminal resistances of the transistor.

The effect of kink is more pronounced when the device is operated at elevated temperatures. Frick et al [3] have observed this effect for a single AlGaAs/GaAs HBT; however no detailed analysis was reported in their study. The most reliable method to extract temperature dependent HBT parasitic resistances is based on  $s$ -parameters, which involves accurate high frequency measurements over temperature. In this paper for the purpose of accurate HBT modelling we propose a simple technique to extract directly the terminal resistances variation with temperature utilizing the observed kink. It is also shown that the main contribution to the enhanced kink at elevated temperature arises from the temperature

dependence of specific contact resistance in metal/ $n^+$  (or  $p^+$ )-GaAs contacts and from the temperature dependence of low field and high field mobilities associated with the undepleted part of  $n$ -InGaP collector and  $n^+$ -GaAs sub-collector.

## II. EXPERIMENTAL AND ANALYSIS

The layer structure and fabrication for the InGaP/GaAs DHBTs studied is given in [4, 8]. DC and high frequency  $s$ -parameters were carried out using Cascade Microtech's thermal probing system over the temperature range of 298K to 383K using InGaP/GaAs DHBTs with emitter geometry of  $16 \times 20 \mu\text{m}^2$ .

Fig. 1 shows the variation of  $I_C$  and  $I_B$  versus  $V_{BE}$  of a  $16 \times 20 \mu\text{m}^2$  InGaP/GaAs DHBT in the temperature range from 248K to 383K. Under high  $I_C$  and low applied reverse bias (or  $V_{BC} \approx 0$ ) the large voltage drop due to collector resistance ( $R_C$ ) forming the undepleted part of the collector, sub-collector and the contact causes the  $b-c$  junction to become forward biased, which gives rise to an additional  $b-c$  junction current ( $I_{BC}$ ) causing a sharp increase in  $I_B$ . This kink effect is seen to enhance with increasing ambient temperature ( $T_A$ ), however the direction of  $I_{BC}$  is the opposite to that of the conventional  $I_C$  causing  $I_C$  to reduce as depicted in Fig. 1.

One would expect the saturation velocity ( $v_{sat}$ ) to decrease with rise in temperature due to lattice perturbations [5]. Any reduction in  $v_{sat}$  would effectively reduce the peak electric field and increase the undepleted region ( $W_C - X_C$ ) of collector thickness ( $W_C$ ) [6, 7]. The voltage drop in the undepleted collector ( $\approx I_C A (W_C - X_C) / q N_C \mu_n$ ) [6, 7] at high  $I_C$  (low  $V_{BC}$ ) would increase due to electron mobility ( $\mu_n$ ) degradation with  $T_A$  and increase of  $W_C$ . For  $I_C \approx I_O$  and  $V_{BC}$  low, where  $I_O = q A v_{sat} N_C$  is the saturated drift velocity current, the electron density ( $n$ ) exceeds the collector doping density ( $N_C$ ) diminishing the electric field leading to base-pushout. For  $I_C > I_O$ , the potential drop across undepleted base ( $R_B$ ) eventually becomes significant limiting the  $b-c$  forward bias. The latter is the reason for the second saturation observed in  $I_B$  as depicted in Fig. 1.

Now if one applies sufficient large reverse bias to the  $b-c$  junction, the electric field on the collector side of the SCR would increase with  $V_{CRIT}$  pushed forward diminishing the observed kink on  $I_B$  as depicted in Fig. 2. The measured  $I_B$  characteristics for  $T = 298\text{K}$  and  $343\text{K}$  under zero and reverse bias conditions are shown in Fig. 2.

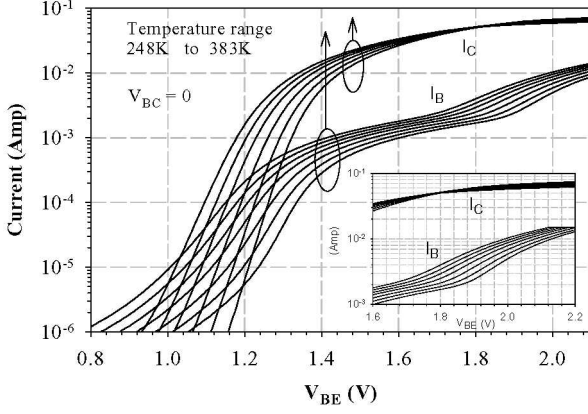


Fig. 1: Variation of Gummel plots with temperature for an InGaP/GaAs DHBT showing the effect of kink on  $I_B$ . The inset shows the reoccurrence of  $I_B$  characteristics at higher  $V_{BE}$ .

From Fig. 2, two observations on  $I_B$  with temperature can be made. Firstly, current gain ( $\beta$ ) of the device at  $V_{BE} = 1.8V$  varies from  $h_{FE} = 25$  (when  $V_{BC} = 0V$  and  $T = 298K$ ) to  $h_{FE} = 22$  (when  $V_{BC} = 1.2V$  and  $T_A = 343K$ ). The temperature dependence of saturation currents in DHBTs generally is complicated due to the fact that both base transport and  $b-e$  and  $b-c$  barrier transport limitations may be important. Bearing this in mind, we attribute this increase in the  $I_B$  to activation energies and pre-exponential terms associated with saturation current components of  $I_B$  [5].

Secondly,  $h_{FE} = 16$  (when  $V_{BC} = 0V$  and  $T = 343K$ ) indicating  $\beta$  drop due to an extra current component ( $I_{BC}$ ) flowing at elevated temperatures, which adds to  $I_B$  causing the onset of the kink to shift to lower  $V_{BE}$ . As discussed this phenomenon was attributed to the  $v_{sat}$  and temperature dependence of  $\mu_n$  associated with  $R_C$  and  $R_B$ . Furthermore, in this region of interest the variation of  $I_C$  is independent of temperature as depicted in Fig. 1; therefore one could eliminate the possibility of any contributions resulting from the temperature dependence of  $I_C$  on  $V_{BE}$ .

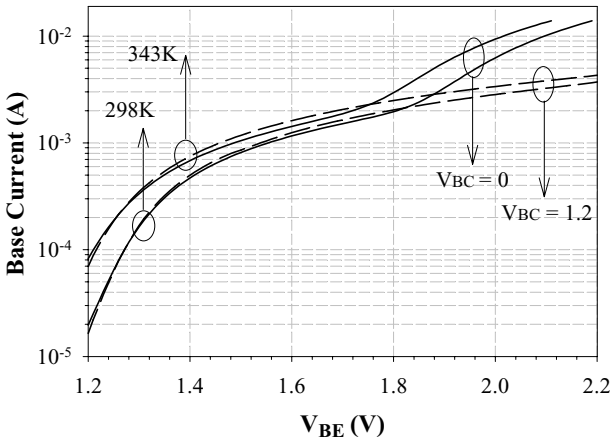


Fig. 2: Measured  $I_B$  vs.  $V_{BE}$  at  $T = 298K$  and  $343K$  under zero and reverse bias conditions.

### III. THEORETICAL MODEL AND EXTRACTION

According to the Ebers-Moll DC model for the bipolar transistor, at medium to high currents,  $I_B$  and  $I_C$  can be expressed as:

$$I_B(T) = I_{BES}(T) \cdot \exp\left(\frac{V_{B'E'}}{n_{BE}(T) \cdot V_T}\right) + I_{BCS}(T) \cdot \exp\left(\frac{V_{B'C'}}{n_{BC}(T) \cdot V_T}\right) \quad (1)$$

$$I_C(T) = I_{CCS}(T) \cdot \exp\left(\frac{V_{B'E'}}{n_{CC}(T) \cdot V_T}\right) - I_{BCS}(T) \cdot \exp\left(\frac{V_{B'C'}}{n_{BC}(T) \cdot V_T}\right) \quad (2)$$

Where  $n_{BE}(T)$ ,  $n_{CC}(T)$  and  $n_{BC}(T)$  are the ideality factors of  $b-e$  current ( $I_{BE}$ ), collector current ( $I_C$ ) and  $b-c$  current ( $I_{BC}$ ) respectively. The actual internal junction potentials  $V_{B'E'}$  and  $V_{B'C'}$  should be corrected by taking into account of the emitter ( $R_E$ ), collector ( $R_C$ ) and base ( $R_B$ ) resistances accordingly as:

$$V_{B'E'} = V_{BE} - R_E I_E - R_B I_B \quad (3)$$

$$V_{B'C'} = V_{BC} + R_C I_C - R_B I_B \quad (4)$$

From the measured base current characteristics of Fig. 2 if one subtracts  $I_B$  from the  $I_B$  in which the kink is observed at any given temperature ( $\Delta I_B(T) = I_B(T, V_{BC} = 0) - I_B(T, V_{BC} > 0)$ ), then the resultant difference should equal to the second term of (1), which gives

$$\Delta I_B(T) = I_{BCS}(T) \cdot \exp\left(\frac{V_{BC} + I_C \left(R_C - \frac{R_B}{\beta(T, I_C)}\right)}{n_{BC}(T) \cdot V_T}\right) \quad (5)$$

If  $\Delta I_B(T)$ 's for different  $T$ 's are plotted logarithmically against  $I_C$ , the graphs will show exponential behaviors (straight lines) in the medium  $I_C$  range as shown in Fig. 3. According to (5) the straight lines fitted to the log ( $\Delta I_B$ ) vs.  $I_C$  plots for different temperatures have a slope of  $(R_C - (R_B/\beta)) / (n_{BC} \cdot V_T)$ , where at moderate  $I_C$ ,  $\beta > 10$ .

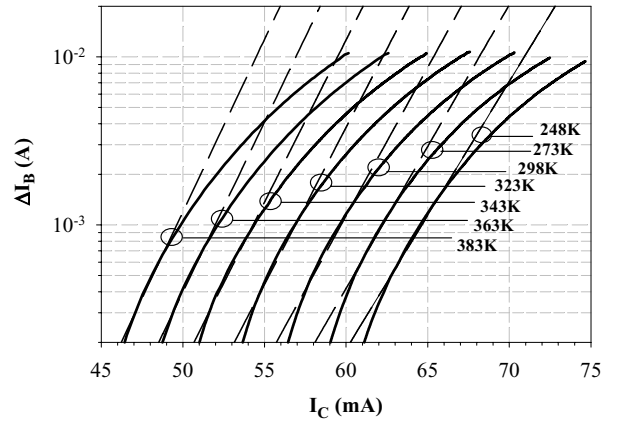


Fig. 3: Plots of  $\Delta I_B (I_B (V_{BC} = 0) - I_B (V_{BC} < 0))$  vs.  $I_C$ . The dashed lines are fits to the exponential regions.

Therefore in the moderate  $I_C$  range,  $(R_B/\beta)$  can be neglected, the slopes of  $\Delta I_B$  vs.  $I_C$  will yield  $R_C$  if the temperature dependence of  $n_{BC}$  is known. It is also shown

in Fig. 3 that with  $I_C$  increasing  $\beta$  will eventually decrease making  $R_B$  significant in the slope of  $\Delta I_B$  vs.  $I_C$ .

When extracting  $R_C$  in the moderate  $I_C$  range care must be taken due to sensitivity of this region. The lines fitted must be in the linear region of the observed kink on  $I_B$ . For this particular device the linear range of kink on  $I_B$  varies from  $I_C = 55 - 64\text{mA}$  at  $T = 298\text{K}$  to  $I_C = 43 - 47\text{mA}$  at  $T = 383\text{K}$ .

In the DHBTs, the conduction and valance band discontinuities ( $\Delta E_C$  and  $\Delta E_V$ ) generated at the junctions will have an important role in tunneling transport mechanisms at high temperature. To correct for this effect the temperature dependence of  $n_{BC}$  need to be taken into account when extracting terminal resistances in (5). As discussed in the previous section using Fig. 2, (4) can be rewritten to include the Kirchoff's current components of  $I_B$  generated at the onset of junction potential reversal.

$$V_{B'C'} = V_{BC} - R_C I_{BC} - R_B I_{BE} + I_C R_C \quad (6)$$

Where  $I_{BC} (= I_B - I_{BE})$  is the current generated at the onset of the kink, the corresponding voltage at which this kink occurs is given as  $V_{KINK}$ . Under moderate  $I_C$ ,  $I_{BE}$  dominates and at high  $I_C$ ,  $I_{BC}$  dominates. The  $R_C I_{BC}$  term of (6) becomes significant due to the potential drop across  $R_C$  forward biasing the b-c junction.

At the onset of the kink, the forward biasing of the b-c junction can be approximated as:  $V_{BC} = V_{BCO} + \Delta V_{BC} = V_{BCO} + \Delta V_{BE}$ , where  $\Delta V_{BE}$  is the difference ( $V_{BE} - V_{KINK}$ ) and  $V_{BCO}$  is a constant. It is noted that  $(V_{BC} = V_{C'} - V_B) = ((V_C - R_C I_C) - V_B)$ , knowing that  $V_C$  and  $R_C$  are constants and  $I_C$  is approximately constant in this region as depicted in Fig. 1. This gives  $V_{BC} (\Delta V_{BC}) \approx \Delta V_{BE}$ . When one observes the kink then  $I_{BE}$  becomes negligible. Hence  $I_B \approx I_{BC}$ , which approximate (5) as:

$$\Delta I_B = I_{BC} = I_{BCO} \cdot \exp\left(\frac{I_{BC} R_C (\beta - 1)}{n_{BC} \cdot V_T}\right) \cdot \exp\left(\frac{\Delta V_{BC}}{n_{BC} \cdot V_T}\right) \quad (7)$$

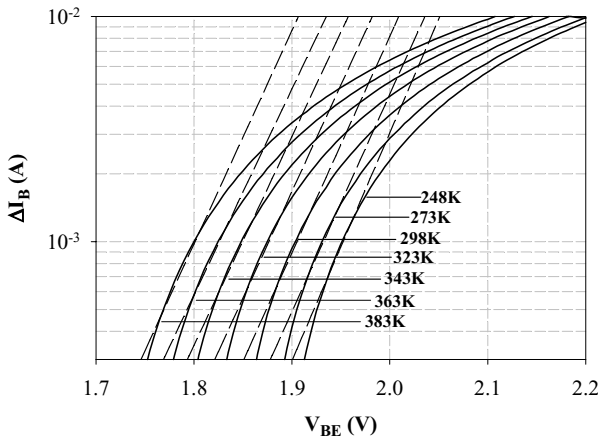


Fig. 4: Plots of  $\Delta I_B (I_B (V_{BC} = 0) - I_B (V_{BC} < 0))$  vs.  $V_{BE}$ . The dashed lines are fits to the exponential regions.

As demonstrated in Fig. 4 if  $\Delta I_B$ 's are plotted logarithmically against  $\Delta V_{BC} (V_{BE} - V_{KINK})$  for each temperature the plots will show exponential behaviors in the moderate  $I_C$  range, the gradient of the best-fit line of each curve will yield  $n_{BC}$ . When extracting ideality

factors ( $n$ ), it is important to identify a common range of  $I_B$  where the log  $I$  versus  $V$  curves are straight lines. It is useful to plot ideality factor ( $n = I_B/kT^*(\Delta V_{BE}/\Delta I_B)$ ) versus  $I_B$  to identify the region where  $n$  is flattest.

Once  $n_{BC}$  and  $R_C$  are known, then one can utilize the plot of  $\Delta I_B$  vs.  $\Delta V_{BC}$  to extract  $R_B$  of the device. For a known  $\Delta I_B$  (or  $I_{BC}$ ),  $\Delta V_{B'C'}$  can be found from a straight line fit to the low current range in the logarithmic plot of  $\Delta I_B$  vs.  $\Delta V_{BC}$ . From (4) it can be given as:

$$I_B = \frac{R_C I_C + \partial \Delta V_{BC}}{R_B} \quad (8)$$

Where  $\partial \Delta V_{BC}$  is the difference  $\Delta V_{BC} - \Delta V_{B'C'}$ . If one plots  $R_C I_C + \partial \Delta V_{BC}$  against  $I_B$  the gradient will yield  $R_B$  at each temperature. Similarly  $R_E$  can be extracted from the Gummel plot when one does not observe the kink ( $V_{BC} > 0$ ), where the second term of (2) can be neglected. For a known  $I_C$ ,  $V_{B'E'}$  can be found from a straight line fit to the moderate  $I_C$  range in Fig. 1. The difference  $\Delta V_{BE} (= V_{BE} - V_{B'E'})$  is plotted against  $I_E (= I_B + I_C)$ , where (3) can be written as  $\Delta V_{BE} = I_E (R_E + R_B^* (1/\beta + 1))$ . This plot should be a straight line and if  $\beta > 10$ , the slope of the line will give  $R_E$ .

#### IV. RESULTS & DISCUSSION

The extracted  $R_C$ ,  $R_B$  and  $R_E$  from the observed kink effect were compared with those deduced from a small signal  $s$ -parameter extraction technique [8]. The extracted values are depicted in Fig. 6. Over the temperature range studied  $R_C$  rose by 30% (dc) and 22% ( $s$ -parameter).  $R_B$  rose by 10% (dc) and 18% ( $s$ -parameter). It was noted that  $R_E$  did not change with varying temperature. From the measured specific contact resistances using TLM measurements at room temperature when calculated gave  $R_E = (9.1 \pm 0.7)\Omega$ ,  $R_B = (29.4 \pm 1.2)\Omega$  and  $R_C = (10.5 \pm 0.6)\Omega$ . These are in close agreement with the terminal resistances extracted from  $s$ -parameter data, indicating that the main contribution is related to the contact resistances.

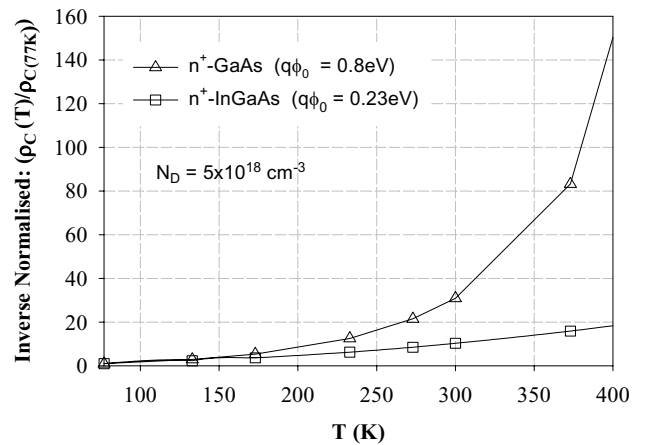


Fig. 5: Variation of normalized specific contact resistance with temperature for metal/ $n^+$ -GaAs and Metal  $n^+$ -InGaAs.

The effect of temperature on contact resistance was analyzed using a theoretical model for tunneling through metal-semiconductor barriers using the Fermi-Direc statistics and WKB approximation [9]. The simulated results of specific contact resistance showed that at 300K, the difference in temperature variation of metal/ $n^+$ -GaAs contact with respect to values at 77K is twice that of metal/ $n^+$ -InGaAs contact. This difference increased by a factor of 4 at 375K as shown in Fig. 5.

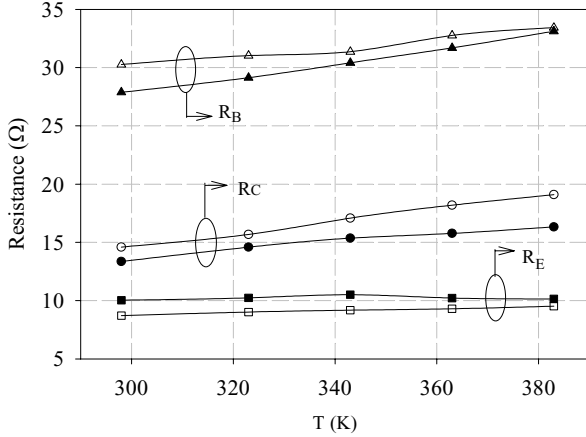


Fig. 6: Variation of measured  $R_E$ ,  $R_C$  and  $R_B$  from  $s$ -parameter extractions (solid symbols) and from the observed kink (open symbols) over the temperature.

From Fig. 6, it is clearly seen that  $R_E$  does not change with varying temperature since the InGaAs cap layer is highly doped. The tunneling current through the barrier formed by InGaAs and metal is very slightly temperature dependent. The  $R_C$  variation with temperature can be explained due to temperature sensitivity of metal/ $n^+$ -GaAs contact and the lightly doped collector not being fully depleted. As a result the decrease in electron mobility of the undepleted InGaP collector and GaAs sub collector can contribute to this variation. The base layer is usually thin. The  $R_B$  variation can mainly result from the temperature dependence of metal/ $n^+$ -GaAs contact. By incorporating these values into a temperature-dependent DHBT large signal model more accurate thermal prediction of  $I_B$  at high currents is demonstrated in Fig. 7.

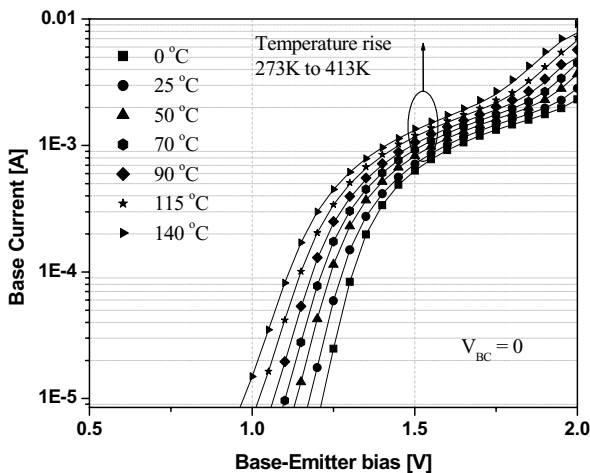


Fig. 7: Measured and simulated  $I_B$  characteristics at various temperatures for a  $16 \times 20 \mu\text{m}^2$  DHBT.

## V. CONCLUSION

We showed a simple and efficient method to extract terminal resistances of DHBTs using the observed kink effect. These data were determined with adequate accuracy and verified by  $S$ -parameter extraction technique. Temperature dependence of terminal resistances was investigated from 298K to 383K. The results show positive coefficient of  $R_C$  and  $R_B$ , which can be originated from the specific contact resistance of metal/ $n^+$ -GaAs and temperature dependence of low field and high field mobilities associated with the undepleted and depleted collector thickness of  $n$ -InGaP collector and  $n^+$ -GaAs sub-collector. These features should be accounted for when modeling DHBT's.

## REFERENCES

- [1] K. Fricke, H. L. Hartnagel, W. Y. Lee and J Wurfl, "AlGaAs/GaAs HBT for High-Temperature Applications," IEEE Trans. Electron Devices, vol. 39, no. 9, pp.1977-1981, September 1992.
- [2] M. Sotoodeh, A. H. Khalid and A. A. Rezazadeh, "DC Characterisation of HBTs Using the Observed Kink Effect on the Base Current," Solid-State Electronics, vol. 42, no. 4, pp. 531-539, 1998.
- [3] S. Tiwari, "A New Effect at High Currents in Heterostructure Bipolar Transistors," IEEE Electron Device Letters, vol. 9, no. 3, pp. 142-144, March 1988.
- [4] M. Sotoodeh, A. H. Khalid and A. A. Rezazadeh, "Empirical Low-Field Mobility model for III-V Compounds Applicable in Device Simulation Codes," Journal of Applied Physics, vol. 87. pp. 2890 -2900, 2000.
- [5] D. A. Ahmari, G. Raghavan, Q. J. Hartmann, M. L. Hattendorf, M. Feng and G. E. Stillman, "Temperature Dependence of InGaP/GaAs Heterojunction Bipolar Transistor DC and Small-Signal Behavior," IEEE Trans. Electron Devices, vol. 46, no. 4, pp. 634-640, April 1999.
- [6] P. Mushini, K. P. Roenker, "Simulation Study of High Injection Effects and Parasitic Barrier Formation in SiGe HBTs Operating at High Current Densities," Solid-State Electronics, vol. 44, pp. 2239-2246, September 2000.
- [7] B. Mazhari and H. Morkoc "Effect of Collector-Base Valence Band Discontinuity on Kirk Effect in Double-Heterojunction Bipolar Transistors," Appl. Phys. Lett. vol. 59, no. 13, pp. 2162-2164, October 1991. , vol. 46, no. 4, pp. 634-640, April 1999.
- [8] M. Sotoodeh, L. Sozzi, A. Vinay, A H Khalid, Z Hu, A. A. Rezazadeh and R. Menozzi, "Stepping Towards Standard Methods of Small-Signal Parameter Extraction for HBT's," IEEE Trans. Electron Devices, vol.47, no.6, pp. 1139 – 1150, June 2000.
- [9] F. A. Amin, A. A. Rezazadeh and S. W. Bland, "Non-Alloyed Ohmic Contacts Using MOCVD Grown  $n^+$ - $\text{In}_x\text{Ga}_{1-x}\text{As}$  on GaAs," Materials Science & Eng, Rev B, pp.195-198, 1999.